Delft University of Technology

Fractality of pulsatile flow in speckle images

Nemati, M.; Kenjeres, S.; Urbach, H. P.; Bhattacharya, N.

Important note
To cite this publication, please use the final published version (if applicable).
Please check the document version above.

Fractality of pulsatile flow in speckle images

M. Nemati, S. Kenjeres, H. P. Urbach, and N. Bhattacharya

Fractality of pulsatile flow in speckle images

M. Nemati,[1] S. Kenjeres,[2] H. P. Urbach,[1] and N. Bhattacharya[1]

[1]*Department of Imaging Physics, Delft University of Technology, Delft, The Netherlands*
[2]*Transport Phenomena Section, Department of Chemical Engineering, Faculty of Applied Sciences and*
J. M. Burgerscentrum for Fluid Mechanics, Delft University of Technology, Delft, The Netherlands

The scattering of coherent light from a system with underlying flow can be used to yield essential information about dynamics of the process. In the case of pulsatile flow, there is a rapid change in the properties of the speckle images. This can be studied using the standard laser speckle contrast and also the fractality of images. In this paper, we report the results of experiments performed to study pulsatile flow with speckle images, under different experimental configurations to verify the robustness of the techniques for applications. In order to study flow under various levels of complexity, the measurements were done for three *in-vitro* phantoms and two *in-vivo* situations. The pumping mechanisms were varied ranging from mechanical pumps to the human heart for the *in vivo* case. The speckle images were analyzed using the techniques of fractal dimension and speckle contrast analysis. The results of these techniques for the various experimental scenarios were compared. The fractal dimension is a more sensitive measure to capture the complexity of the signal though it was observed that it is also extremely sensitive to the properties of the scattering medium and cannot recover the signal for thicker diffusers in comparison to speckle contrast. *Published by AIP Publishing.* [http://dx.doi.org/10.1063/1.4948297]

I. INTRODUCTION

The transmission or reflection of coherent light through diffuse media gives rise to a granular intensity pattern called speckle. The different optical path lengths traversed by coherent light in a medium leads to constructive or destructive interference in the image plane. The image contains bright or dark spots of varying sizes and intensity. Laser light illuminating a rough surface is an ideal scenario for generation of speckle. This is noise for most imaging applications but carries valuable information about the medium. By studying the changes in the speckle pattern, the time evolution of the medium can be observed. In case the object as a whole moves or parts of it move, changes can be seen in the speckle pattern that are correlated to the motion for a certain time, till the speckle pattern decorrelates completely. This offers a unique opportunity to study changes in a medium without direct imaging by simply quantifying the decorrelation in the speckle pattern. The coarseness in granularity of the spatial intensity distribution of the speckle patterns makes them good candidates for a study of fractality.[1] The study of fractals in nature can vary from studying coastlines, heartbeats, and snowflakes to the capillary network in lungs.[2,3] The fractal classification can vary depending upon the object of study. One major distinction can be made between regular or exact fractals and random or statistical fractals. A regular fractal is defined when the object is an exact replica of itself and appears self-similar on different scales, whereas an object is a statistical fractal when its statistical properties replicate at different scales. Many physical systems show that the characteristics of being statistical fractals and scattering of coherent light from diffuse media to form speckles also fall in this category. The random spatial distribution of bright and dark spots in a speckle image displays the self-similarity, scaling, and statistics which we are familiar with in fractals.[4] Fractal statistics is also very relevant in studying biological systems. For example, in a living system, a certain level of complexity is considered normal and any deviation from that behavior can indicate disease.[5] In most physiological processes, the measured values usually fluctuate in time and this can also be studied for fractal behavior. This has been investigated in studies like that of cardiac inter-beats for healthy volunteers and patients.[6] Optical techniques are used in biomedical imaging because important information can be obtained in a non-invasive manner. These techniques can range from point or line scans for instance in optical coherence tomography to the full field imaging techniques. The imaging techniques have their own complex requirements due to the equipment and data processing required. The technique of laser speckle imaging is currently being studied as a method to extract biomedical parameters using indirect imaging.[7–9] *In-vivo* biomedical imaging always has the complication of relative motion between the imaging system, the illumination, and the subject. This is even more relevant when imaging dynamics like flow in a living medium. Speckle based techniques have been shown to be quite robust for such cases.[10,11] In most cases, the sample is illuminated by a laser light and the scattered light is collected by a camera. Due to interference of the light diffracted by the scatterers in the diffuse media, a grainy speckle image is created. In the cases where the sample is subject to motion or contains moving particles, the dynamics of the complex scattering medium can be extracted from the time evolving speckle patterns. The complexity of these signals is mainly due to fluctuations caused by moving red blood cells (RBCs) and appears to be quite random in a scattering medium such as in the skin with an

underlying capillary network. The standard technique of studying these dynamic series of speckle patterns is based on spatial or temporal implementations of laser speckle contrast analysis. Fractal statistics is being used to study speckle images in many recent studies.[1,12,13] Analyzing the speckle data with fractal statistics provides a measure of the fluctuations of an evolving process at different temporal resolutions. This reveals the self-similarity and regularities which underlie the apparent chaotic changes in the signal. This behavior where statistical properties of smaller parts are proportional to statistical properties of the whole can be addressed using power law scaling in fractal statistics.

In this paper, we report on a study of a pulsatile flow using speckle images. The characteristics of dynamic speckle patterns generated by a pulsatile flow also fluctuate depending upon where in the time cycle of the pulse the image is acquired. This is also reflected in the fractality of the speckle images. Studying the fractal dimension (FD) of the image also yields crucial information about the underlying flow pulsation mechanism. Here we focus on flow pulsating systems. In every case, the fluid is pulsed at frequencies close to the human heart. For fractal analysis of the speckle images, using the differential box counting approach, we have measured the changes of fractal dimensional over time. The speckle images were measured from different phantoms and with underlying pulsating flow with different scattering fluids. These datasets were in parallel analyzed using standard speckle contrast analysis.

II. METHODS

A. Laser speckle contrast analysis

Study of dynamics in diffuse media using time varying speckle patterns arising due to laser illumination has the advantage of being full field and relatively inexpensive. A speckle pattern generated by a sample which contains moving scatterers gets increasingly blurry as the integration time of the pattern increases. Finally, the patterns decorrelate completely. The crucial information about the evolution of the media can be obtained by analyzing the time fluctuation dynamics of speckle images. Laser speckle contrast was first introduced by Goodman[14] and demonstrated by Briers and Webster[15] as a parameter which can be used to quantify the changes in the medium being studied. The speckle contrast (K) is defined as the ratio of the standard deviation (σ) over the average intensity fluctuation ($\langle I \rangle$), in the image[16,17]

$$K = \frac{\sigma}{\langle I \rangle}. \qquad (1)$$

This parameter can be evaluated for the entire image at once or using a sliding spatial window of (n × n) camera pixels.[18] A pulsatile flow can be studied using speckle contrast by recording a time series of speckle images. The resulting contrast time series are then Fourier transformed to obtain the frequency spectrum. This frequency spectrum has information about all the fluctuations arising in the flowing media for the entire duration of each measurement. This is also a function of the camera exposure time and acquisition rate.

B. Fractal analysis of speckle images

The fractal dimension of an image mainly corresponds to the perception of roughness and also describes the scaling seen in it mathematically. The fragmentation of the image into structures where smaller pieces can reproduce the statistical properties of the entire image shows the measure of fractality. This can be explained using a scaling law, where an image is a union of N distinct, non-overlapping copies of itself. The copies have been scaled down by a ratio r = M/s, where M is the image size and s is the size of the length scale of the composing copies. The number N is related to the ratio by

$$N(s) \cong r^{-D}, \qquad (2)$$

where the non-integer exponent D is the fractal dimension. It has been shown that the fractal dimension can be a useful tool to study complex systems. The estimation of the fractal dimension (FD) of an image can be performed using several techniques: the Fourier power spectrum of image intensity,[19] the triangular prisms, or the reticular cell counting method[20,21] depending upon what is being investigated. These techniques can be classified under three main categories of the spectral methods, the variance methods, and finally the box counting methods.[22] The study of certain properties that do not change as an object undergoes continuous deformation is described by topological dimension. This is represented by the Koch snowflake where the topological dimension stays the same even as the curve gains more complexity.[23] However, the fractality of the curve can reveal another dimension which mainly reflects the properties of the evolving curves and characterizes their texture. This is a good measure of how structure or coarseness is distributed in a surface area and can be clearly related to the spatial distribution measured in a speckle pattern. The time evolution of this in the area under observation is very useful in studying dynamical systems. The original term fractal was used to describe objects whose Hausdorff-Besicovitch dimension exceeded their topological dimension. However, Mandelbrot applied this term for all sets of objects which were self-similar, self-affine, or quasi-self-similar.[24] The concept of self-similarity can also be applied to the temporal evolutions. The essential properties of fractals are often seen in speckle images. In a speckle image, a large number of wavelets contribute to form a dark or bright spot in the image plane. The contributing waves have encountered various path lengths on the surface or inside the medium. In case of the box-counting method, the fractal dimension is computed by subdividing the speckle image with multiple boxes of a specific size as seen in Fig. 1 and by estimating how many of them are required to cover the whole object.[25] This process is repeated for a range of sizes. If the number of boxes N(s) is estimated across a range of s, then there should be linear relationship between log(N(s)) and log(1/s), where the measured slope is an indication of the fractal dimension. The fractal dimension then can be written as
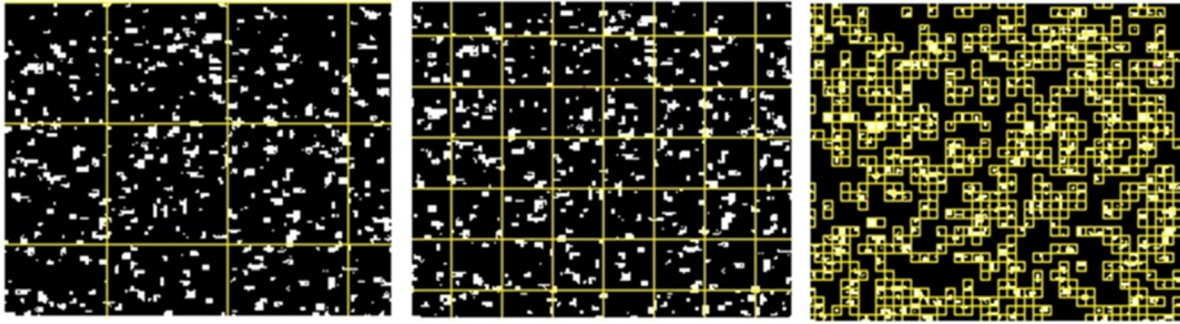
FIG. 1. Box counting for a typical speckle image which has been converted to a fractal image. Three different values of the box size are shown.

$$FD = \lim_{s \to 0} \frac{\log(N_s)}{\log(1/s)}.$$ (3)

The original idea of box counting has been extended to differential box counting by considering an image as a surface where its height is proportional to its image gray value or intensity.[26] In our analysis, the differential box counting has been carried out on the speckle images to extract the fractal dimension. An example of the speckle image recorded with pulsatile flow is shown in Fig. 2, along with the image transformed into the corresponding fractal image.

In this work, a speckle image is considered as a 3D spatial surface where two coordinates are the spatial coordinates of the pixel and the third one is the gray level. The original speckle images are transformed to the fractal images. For differential box counting, an image of size M divided into 3D space blocks (s x s x s'), where s is the size of the square and s' is the gray level of the block. If the total gray level of the image is G, then we can write $G/s' = M/s$. To determine the required thickness of the blanket needed to cover the image surface, we need to know that the minimum gray level falls in the box number k and the maximum gray level falls into box number l. Then the thickness of the blanket coverage on the grid (i, j) is

$$n_s(i,j) = l - k + 1.$$ (4)

The total number of boxes is calculated for different values of s, as

$$N_s(i,j) = \sum_{\substack{1 \le i \le M/s \\ 1 \le j \le M/s}} n_s(i,j).$$ (5)

The fractal dimension was calculated for each image from the slope of the linear regression line fit to the log plot of total number of boxes N_s versus the dimension scale or the box size s. This approach is mainly used in medical setting for feature extraction.[27] To study dynamics, a time series of fractal dimension has been used to determine the corresponding frequency spectrum.

III. EXPERIMENTAL SETUPS

In this section, an overview of different parts of the setup will be given. The basis of the experimental setup itself is simple and can be decomposed into three main parts: illumination, detection, and phantom with a scattering fluid having pulsatile flow. In practice, the measurements were carried out in different experimental settings using various phantoms and pumping mechanisms to generate the pulsation in the fluid. The main purpose was to test the general technique and analysis algorithms for robustness in a variety of real life situations. The phantoms are shown in Fig. 3, and they consist of a rectangular flow cell, a cylindrical phantom, and a carotid artery phantom. For all cases, the detection was performed using a high speed camera (Photron Fastcam SA3) with the pixel size of $17 \times 17 \, \mu$m. The camera exposure time is 20 ms and the frame rate is 50 Hz. For illumination, in the case of the rectangular flow cell, we used a He-Ne laser at 633 nm; for the cylindrical phantom and the carotid artery phantom, we used a frequency doubled Nd:YAG laser at 532 nm to directly illuminate the sample. The pulsatile flow has been studied in three different experimental settings which are associated with different phantoms as will be explained in more details at each measurement section.
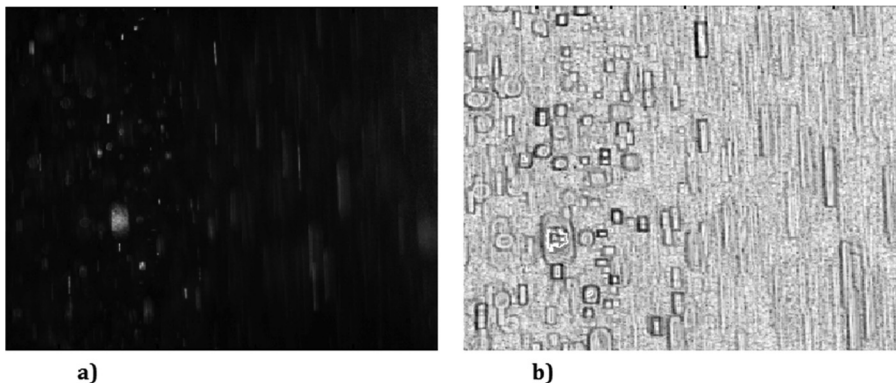

a)   b)

FIG. 2. (a) Raw speckle image of pulsatile flow in the cylindrical phantom. (b) The speckle image converted to corresponding fractal image.
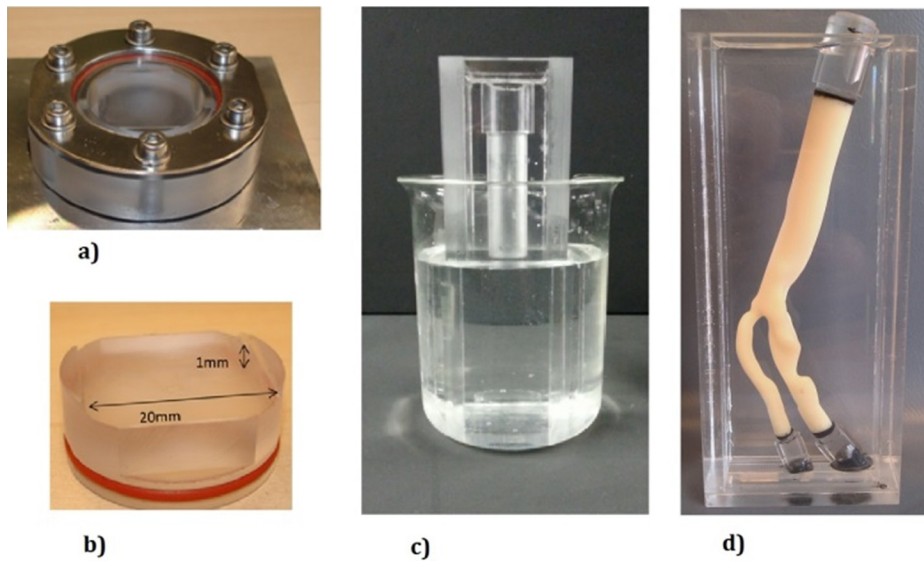
FIG. 3. The different phantoms which have been used for the experiments. (a) Flow cell which can be fitted with different top membranes to introduce static scatterers. (b) The insert into the flow cell to mimic a homogeneous thin layer of flow. (c) Cylindrical phantom showing the effect of index matching using glycerol solution. (d) Carotid artery phantom showing the bifurcation.

The results of the measurements are summarized in three different sections, to study the influence of: the static scatterers, a complex pulsatile flow, and *in-vivo* measurements.

A. Static scatterers

These experiments were carried out using a semi-rectangular channel phantom. As shown in Figs. 3(a) and 3(b), the flow cell consists of a semi-rectangular channel with a length of 20 mm and a depth of 1 mm to represent a homogeneous, thin layer of flow. The top membrane of the cell can be interchanged to be a glass or a non-transparent skin phantom made of Delrin® (polyoxymethylene, POM) to mimic the scattering properties of skin.[28] In this experiment, we used a roller pump (Minipuls® 3) to generate a pulsatile

flow with a controlled frequency in our sample. The fluid used with this phantom was milk, which like blood is a bulk scatterer and has fat particles which have similar scattering properties to red blood cells (RBCs) in blood.[29,30] The measurements aimed to observe the influence of a top membrane and consider the effect of additional static scatterers besides the scattering along the flow on the dynamic speckle images. The three configurations considered included a top membrane of glass, Delrin with 1 mm thickness and 2 mm thickness. The dynamic speckle images were then analyzed, and the results of the time series can be seen in Fig. 4. The analysis using the standard speckle contrast can be seen in Figs. 4(a)–4(c) and using the fractal dimension of the images can be seen in Figs. 4(d)–4(f).
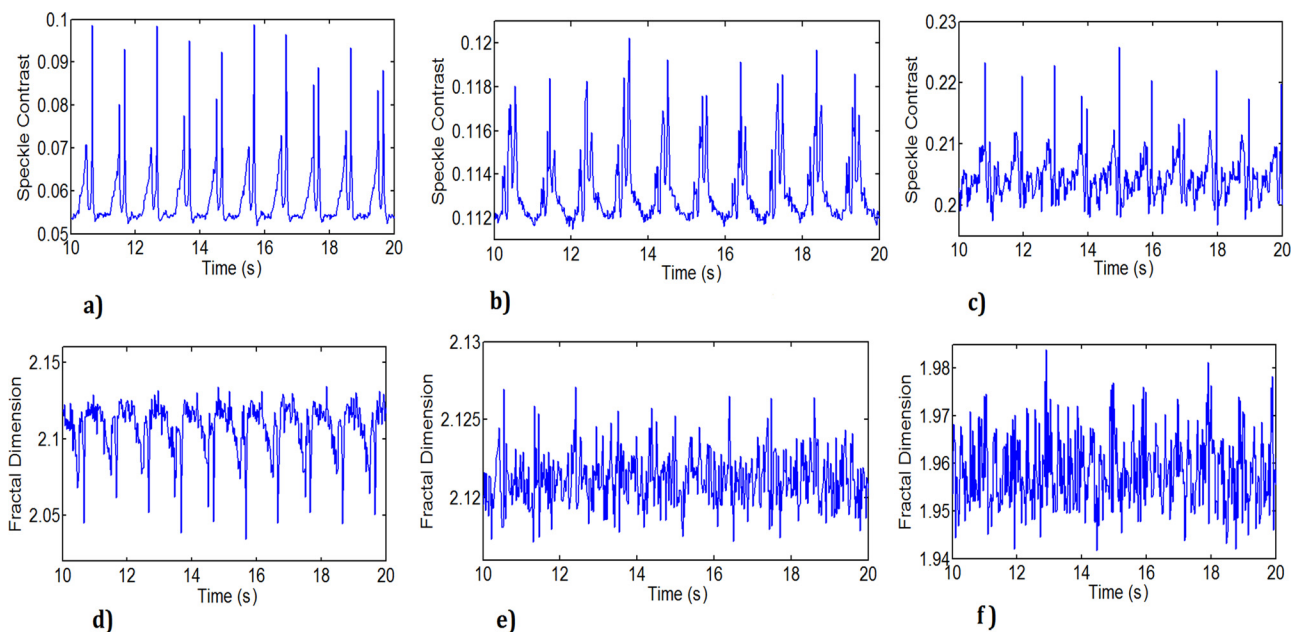

FIG. 4. The time series signal measured for pulsatile flow in the rectangular flow channel with different top membranes. (a) Glass membrane, images analyzed, with speckle contrast. (b) 1 mm thick Delrin membrane, images analyzed, with speckle contrast. (c) 2 mm thick Delrin, images analyzed, with speckle contrast. (d) Glass membrane, images analyzed, with fractal dimension. (e) 1 mm thick Delrin membrane, images analyzed, with fractal dimension. (f) 2 mm thick Delrin membrane, images analyzed, with fractal dimension.

The effects of changes in the velocity of the scatterers and the changes in the particle density in the pulsatile fluid signal leave a different imprint on the contrast and fractal dimension of the images. This can be seen clearly in Fig. 4. The frequency spectrum of the time series data in Fig. 4 is shown in Fig. 5. In the absence of static scatterers in Figs. 4(a) and 4(d), we can see that the time series data are similar, though the bulk scattering in the milk does make the time series of the fractal dimension more noisy. The frequency spectra seen in Figs. 5(a) and 5(d) are very similar. The addition of the extra static scattering layer adds to complexity, but the time series data with laser contrast analysis can still monitor the pulsating flow. The fractal dimension of the images changes more rapidly with the thickness of the layer of static scatterers, to the extent that for thicker layers, they are not able to monitor the pulsating flow. This also reflected in the frequency spectra of the respective time series, though both techniques could determine the primary frequency of pulsation of the pump which was at 1.25 Hz.

B. Pulsatile flow in different phantoms

The second case we studied was with the pulsatile flow generated using the Medos Ventricular Assist Device (VAD), which bears a strong resemblance to a pulsating heart. For the VAD settings, we used a systolic pressure of 270 mmHg and the diastolic pressure of −30 mmHg with a systolic time interval of 35% with a ventricular pump of 60 cm^3. The frequency of the cardiac pulsation is set for 40 beats per min. For pulsating flow conditions, the Reynolds number was between 16 and 512, for diastolic and systolic pressure, respectively. The pulsatile flow results in a lower Reynolds number compared to the steady flow.[30,31]

With this pump, we used two transparent phantoms of different geometry, a cylindrical tube and a carotid artery phantom. This will be described next.

1. Cylindrical phantom

The cylindrical tube phantom, as shown in Fig. 3(c), made of cured Polydimethylsiloxane (PDMS), with outer diameter of 20 mm was used with the VAD as the pumping source. The fluid in this case was an aqueous glycerol solution with the same refractive index, n = 1.413, as the phantom housing. This was done for refractive index matching as can be seen in Fig. 3(c). The glycerol solution is non-toxic and can easily dissolve in water. This eliminates any extra scattering from the phantom itself. To create a scattering fluid which mimics blood flow, we use seeding particles. The hollow glass particles with the diameter size ranging from 4 to 20 μm are main source of scattering of the incoming laser light to create the speckle patterns. If the flow is seeded sufficiently, a speckle pattern will be formed by the collectively scattered light field from the seeding particles. In Fig. 6(a), the time series generated using the speckle contrast analysis on the measured images with a cylindrical phantom can be seen, and in Fig. 6(b), the time series generated using the fractal dimension analysis using the cylindrical phantom can be seen. The rate of pulsation was set to be 0.6 Hz. In comparison to the experiment with the bulk scattering fluid, milk, we observe that in the case of the transparent phantom and low seeding, the change in the fractal dimension has a stronger signature. Again, in both cases, the frequency analysis of the time series reveals the primary frequency of pulsation of the pump of 0.6 Hz.

2. Carotid artery phantom

The carotid artery phantom, Fig. 3(d), was made from a 3D wax print of the artery of a patient suffering from atherosclerosis, using computed tomography (CT) scan images.[32] In this case, we also use an aqueous glycerol solution with the same refractive index (n = 1.413) as the phantom. Due to its complex geometry, the measurements from the phantom of the carotid artery have been analyzed at different locations as indicated in Fig. 7. These locations are the bifurcation in
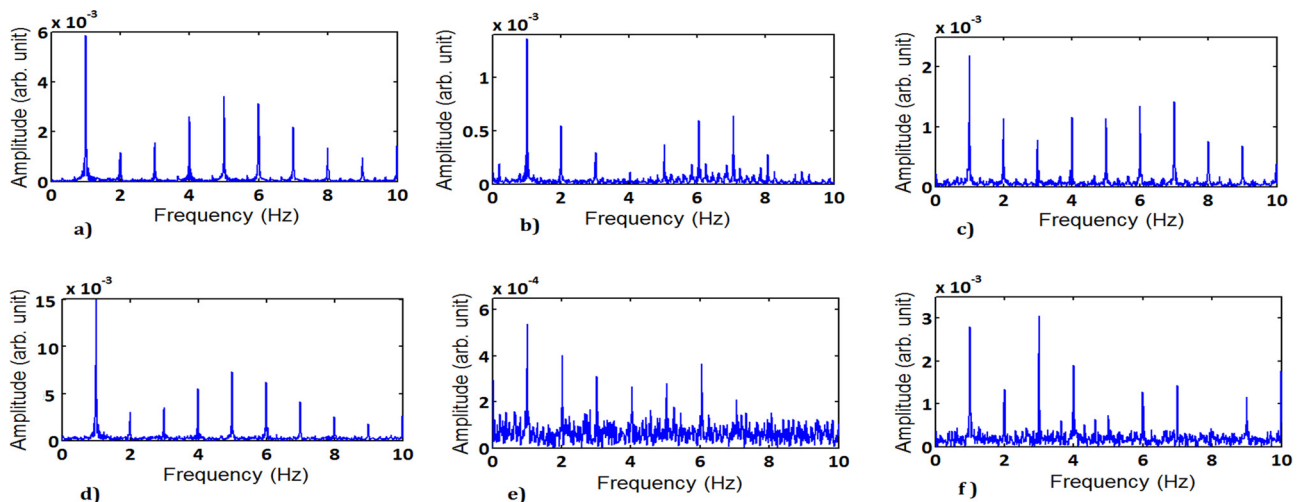

FIG. 5. The spectral analysis of the time series measured for pulsatile flow in the rectangular flow channel with different top membranes. (a) Glass membrane, images analyzed, with speckle contrast. (b) 1 mm thick Delrin membrane, images analyzed, with speckle contrast. (c) 2 mm thick Delrin, images analyzed, with speckle contrast. (d) Glass membrane, images analyzed, with fractal dimension. (e) 1 mm thick Delrin membrane, images analyzed, with fractal dimension. (f) 2 mm thick Delrin membrane, images analyzed, with fractal dimension.
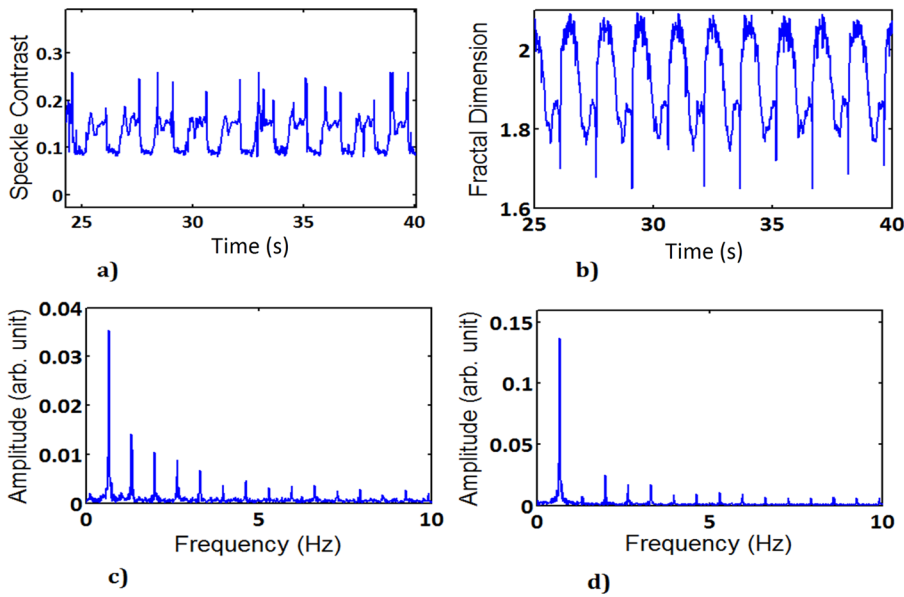
FIG. 6. The time series signal of speckle images from pulsatile flow in the cylindrical phantom. (a) Images analyzed with speckle contrast. (b) Images analyzed with fractal dimension. Spectral decomposition of images analyzed with (c) speckle contrast and (d) fractal dimension, respectively.

common carotid artery (zone 1), stenosis (zone 2) and external carotid artery (zone 3). These are the most common locations for the plaque formation along the carotid artery.[33] Therefore, it is advantageous to study the full system with multiple zones for data analysis, to provide an insight into the flow dynamics. We observe that the flow dynamics is very complicated in this scenario as seen in Fig. 7. The speckle contrast time series as seen in Figs. 7(a)–7(c) and the fractal
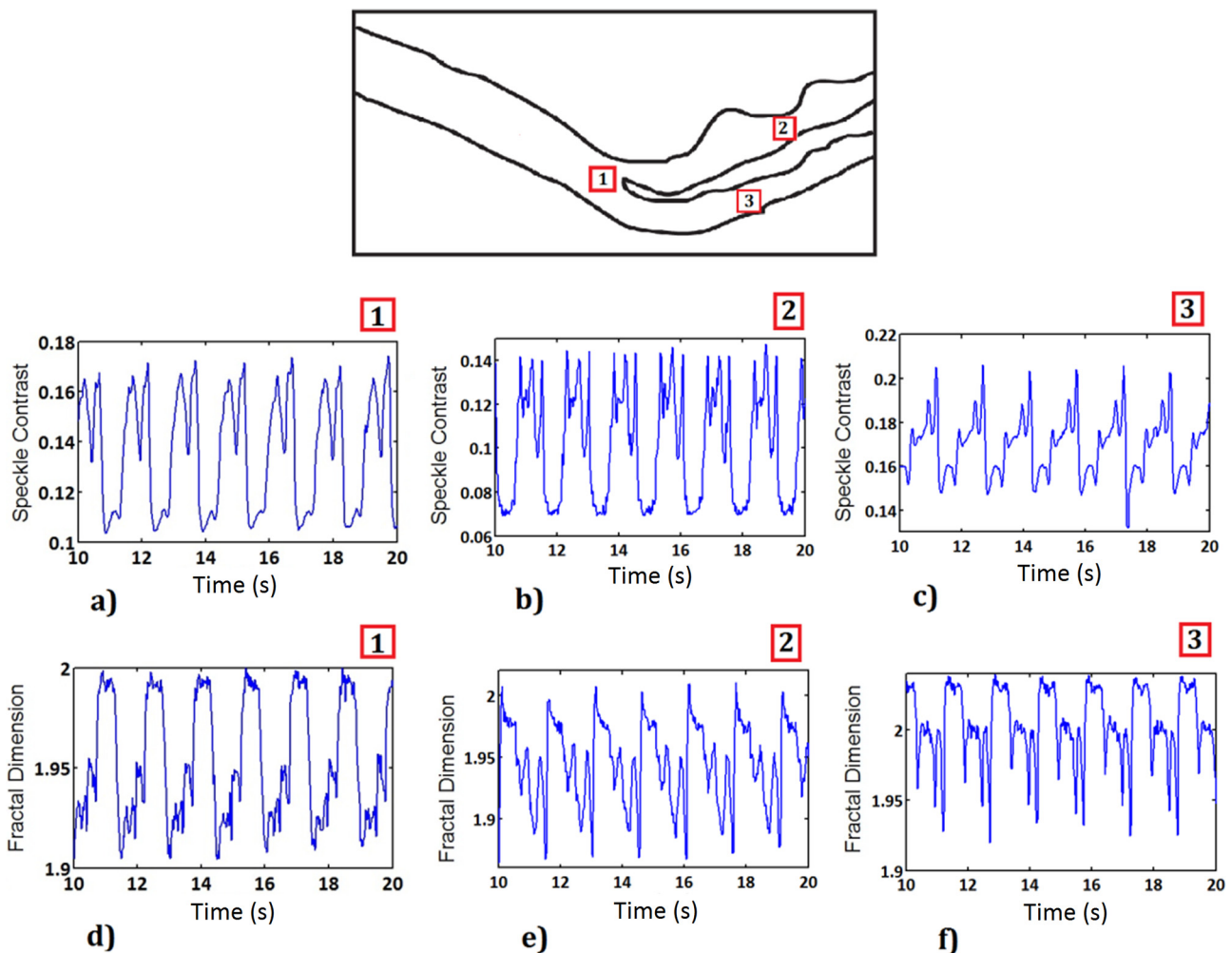

FIG. 7. The time series of speckle images from the three (1, 2 and 3) locations along the carotid artery phantom as shown above. Images analyzed using speckle contrast (a), (b), and (c) for zones 1, 2, and 3 as seen above. Images analyzed using fractal dimension (d), (e), and (f) for zones 1, 2, and 3 as seen above.
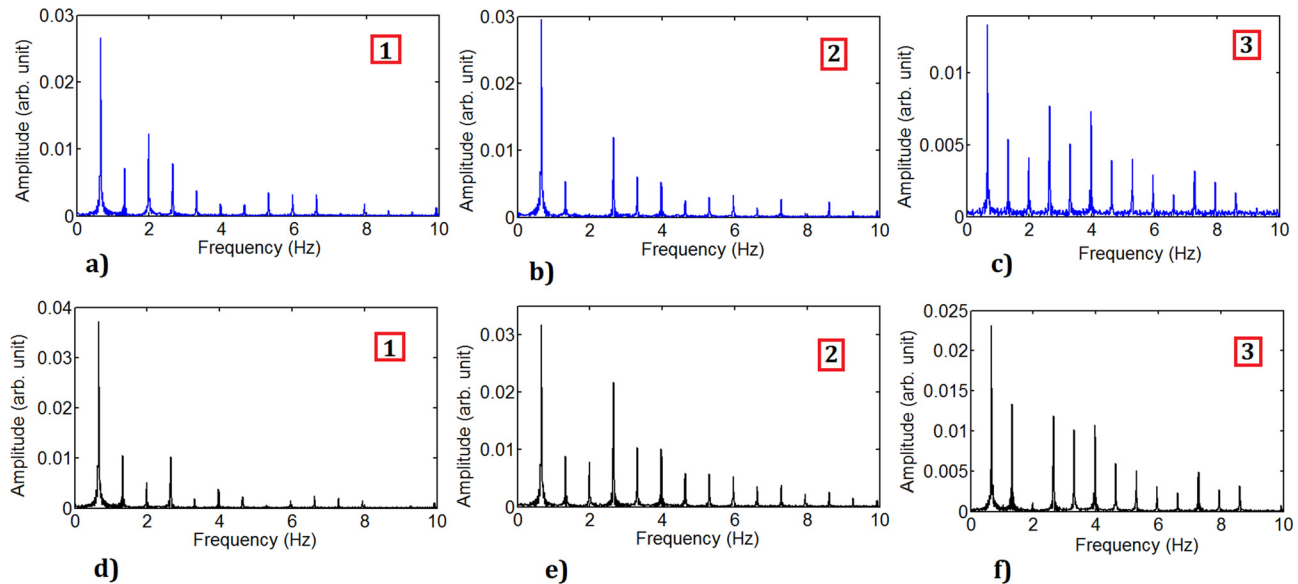
FIG. 8. The spectral analysis of the time series of speckle images from the three (1, 2, and 3) locations along the carotid artery phantom as shown in Fig. 7. Spectra of images analyzed using speckle contrast (a), (b), and (c) for zones 1, 2, and 3 in the phantom. Spectra of images analyzed using fractal dimension (d), (e), and (f) for zones 1, 2, and 3 in the phantom.

dimension time series as seen in Figs. 7(d)–7(f) reflect different aspects of this complexity. The frequency spectrum of the time series seen in Fig. 7 is shown in Fig. 8. The frequencies contributing to the pulse are reflected with different amplitudes in the speckle contrast time series and the fractal dimension time series. It is noted that the spectra using both techniques largely reflect the major contributing frequencies.

3. In vivo *measurements*

The flow pumps in the above two cases maintain a steady pulsation rate; in contrast, a heart changes its pulsation rate. To investigate the feasibility of these techniques

for *in vivo* situations, we investigated the speckle dynamics for blood flow in a volunteer for two different situations. First, we captured the speckle images, in reflection geometry from a volunteer with the laser light illuminating the finger. The results are illustrated in Fig. 9. The time series from a large network of capillaries which give rise to the dynamic speckle in the images can be seen in Fig. 9(a) speckle contrast and Fig. 9(b) fractal dimension. There is a layer of static scattering skin which also contributes to the speckle images. The capillary network also has no unique direction of flow. Thus, we see that though the speckle contrast time series does seem to reflect the pulsating behavior of the underlying blood in the fractal dimension time series, this is not very clear. The frequency analysis of Figs. 9(c) and 9(d) on the
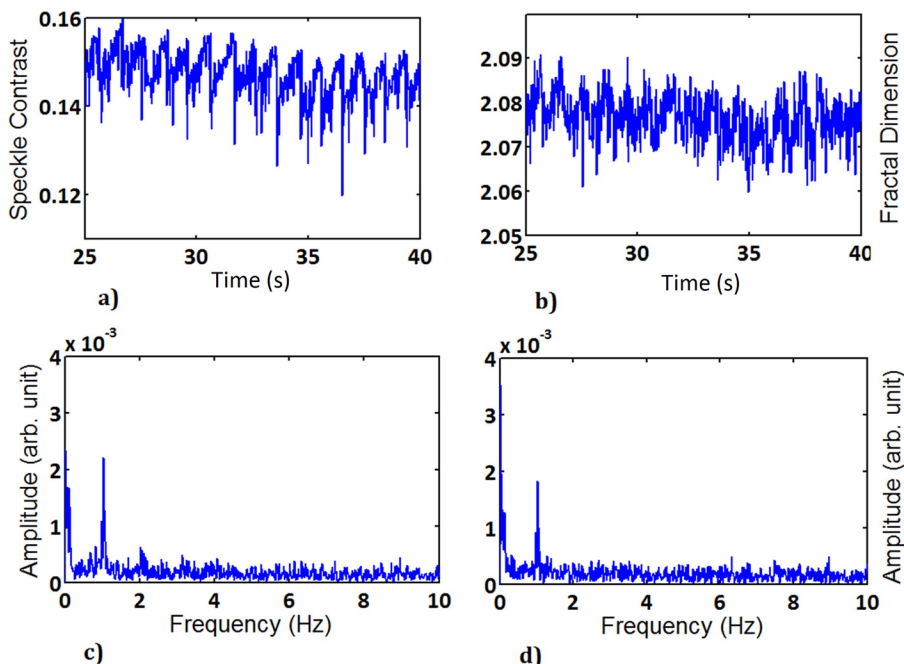

FIG. 9. The time series of speckle images measured from the finger of a volunteer analyzed with (a) speckle contrast and (b) fractal dimension. Spectral analysis of the times series from (c) speckle contrast and (d) fractal dimension.
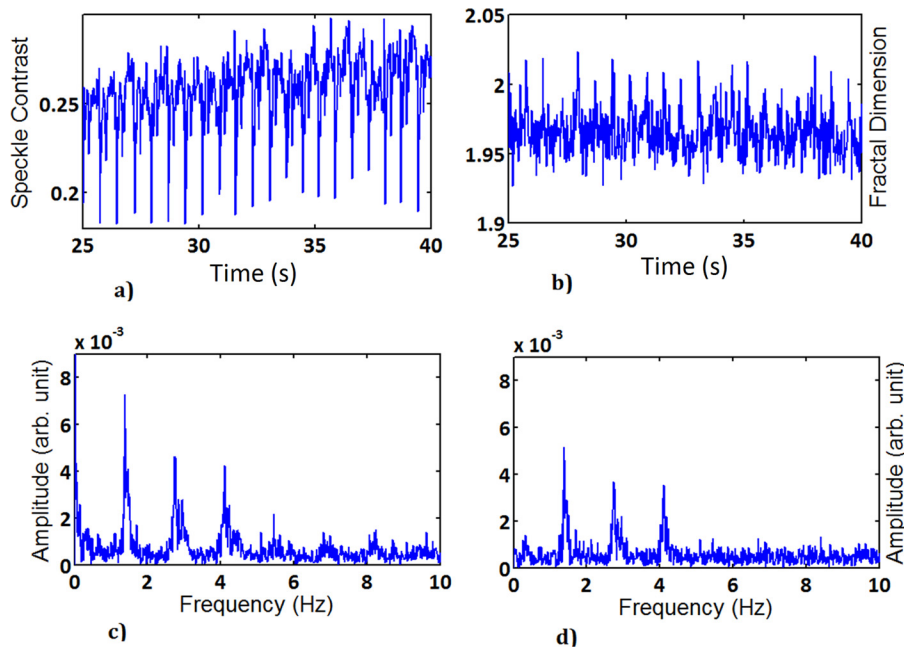
FIG. 10. The time series of speckle images measured from the carotid artery of a volunteer analyzed with (a) speckle contrast and (b) fractal dimension. Spectral analysis of the times series from (c) speckle contrast and (d) fractal dimension.

other hand shows that both techniques capture the principle frequency, which is the heart rate.

The second situation was to record speckle images of the right carotid artery of a volunteer, again in reflection geometry with laser illumination. The results are illustrated in Fig. 10. In this case, again there is a layer of static scattering skin, but the flow direction is unique. The time series for both the speckle contrast and fractal dimension clearly reflect the periodic pulsation in the flow. The frequency analysis of using both time series is also quite similar and captures the principle frequency in both cases. In both the *in vivo* cases, the heartbeats of the volunteer were monitored with a wrist heart rate monitor and correspond to our measurements. Further work is necessary to investigate the possible conditions for devices to work on this principle.

IV. RESULTS AND DISCUSSIONS

The multiscale analysis of time series of light scattered from a sample can be a useful tool for better understanding the complex underlying mechanisms of the medium. In this paper, we studied the fractal dimension change of speckle images of pulsatile flow and compared it to speckle contrast analysis. We address the result of measured fractal dimension for the case of pulsatile flow using different membranes on top of the bulk scattering fluid. We observe that in case of a 2 mm thick layer of Delrin as the top membrane, which has a high number of static scatterers, the fractal dimension does not reflect the pulsation and changes in flow. In contrast to that the laser speckle analysis can still capture the changes in the pulsatile flow. We also studied the speckle images generated by pulsatile flow from a Ventricular Assist Device in a transparent fluid where the scattering was only generated through seeding particles. Here we observe that the two techniques capture different aspects of the complexity of the flow, though in a transparent setting the fractal dimension is more sensitive than laser contrast. Measurements were also performed on a realistic phantom where the flow becomes

complex due to the geometry of the channel. In this case, we observed that even though the rapid changes in the flow leave different imprints on the fractal dimension change and the contrast, the essential frequencies were captured by both techniques. We also attempted to test the method for *in vivo* case and observe that the changes in the fractal dimension and in the contrast of the speckle images manage to capture the heart rate. The fractal dimension is a more sensitive measure than speckle contrast since it can measure the texture of image. It is also extremely responsive to rapid changes in the texture, and this can be exploited to study the time evolution in more complex media just by observing the scattering from it.

ACKNOWLEDGMENTS

[1]G. Steve, M. C. Peron, and E. Delechelle, "Spatial speckle characterization by Brownian motion analysis," Phys. Rev. E **70**(4), 046618 (2004).
[2]B. Mandelbrot, *The Fractal Geometry of Nature* (Henry Holt and Company, 1983).
[3]R. W. Glenny, H. T. Robertson, S. Yamashiro, and J. B. Bassingthwaighte, "Applications of fractal analysis to physiology," J. Appl. Physiol. **70**, 2351–2367 (1991); available at http://www.ncbi.nlm.nih.gov/pmc/articles/PMC4063444/.
[4]R. Correa, J. Meireles, J. Huguenin, D. Caetano, and L. Da Silva, "Fractal structure of digital speckle patterns produced by rough surfaces," Physica A **392**, 869–874 (2013).
[5]J. B. Bassingthwaighte, L. S. Liebovitch, and B. J. West, *Fractal Physiology* (American Physiological Society, 1994).

[6]A. L. Goldberger, L. A. N. Amaral, J. M. Hausdorff, P. C. Ivanov, C. K. Peng, and H. E. Stanley, "Fractal dynamics in physiology: alterations with disease and aging," Proc. Natl. Acad. Sci. U.S.A. **99**, 2466–2472 (2002).

[7]M. Draijer, E. Hondebrink, T. Van Leeuwen, and W. Steenbergen, "Twente optical perfusion camera: System overview and performance for video rate laser Doppler perfusion imaging," Opt. Express **17**(5), 3211–3225 (2009).

[8]M. A. Vilensky, O. V. Semyachkina-Glushkovskaya, P. A. Timoshina, Ya. V. Kuznetsova, I. A. Semyachkin-Glushkovskii, D. N. Agafonov, and V. V. Tuchin, "Laser speckle-imaging of blood microcirculation in the brain cortex of laboratory rats in stress," Quantum Electron. **42**(6), 489–494 (2012).

[9]T. Sugiyama, M. Araie, C. E. Riva, L. Schmetterer, and S. Orgul, "Use of laser speckle flowgraphy in ocular blood flow research," Acta Ophthalmol. **88**, 723–729 (2010).

[10]B. Parthasarathy, W. J. Tom, A. Gopal, X. Zhang, and A. K. Dunn, "Robust flow measurement with multi-exposure speckle imaging," Opt. Express **16**, 1975–1989 (2008).

[11]M. Nemati, R. W. Wijshoff, J. M. Stijnen, S. Van Tuijl, J. W. Bergmans, N. Bhattacharya, and H. P. Urbach, "Laser speckle based detection of fluid pulsation in the presence of motion artifacts: in vitro and in vivo study," Opt. Lett. **38**, 5334–5337 (2013).

[12]O. Carvalho, M. Benderitter, and L. Roy, "Noninvasive radiation burn diagnosis using speckle phenomenon with a fractal approach to processing," Biomed. Opt. **15**(2), 027013 (2010).

[13]C. Lal, A. Banerjee, and N. Sujatha, "Role of contrast and fractality of laser speckle image in assessing flow velocity and scatterer concentration in phantom body fluid," Biomed. Opt. **18**(11), 111419 (2013).

[14]J. W. Goodman, "Some fundamental properties of speckle," J. Opt. Soc. Am. **66**, 1145–1150 (1976).

[15]J. D. Briers and S. Webster, "Quasi real-time digital version of single-exposure speckle photography for full-field monitoring of velocity or flow fields," Opt. Commun. **116**, 36–42 (1995).

[16]J. W. Goodman, *Speckle Phenomena in Optics* (Roberts and Company Publishers, 2007).

[17]J. C. Dainty, *Laser Speckle and Related Phenomena* (Springer-Verlag, 1984).

[18]M. Draijer, E. Hondebrink, T. Van Leeuwen, and W. Steenbergen, "Review of laser speckle contrast techniques for visualizing tissue perfusion," Lasers Med. Sci. **24**(4), 639–651 (2009).

[19]A. P. Pentland, "Fractal based description of natural scenes," IEEE Trans. Pattern Anal. Mach. Intell. **6**(6), 661–674 (1984).

[20]J. Feder, *The Fractal Dimension*, Physics of Solids and Liquids (Springer, 1988) p. 6–30.

[21]B. Klinkenberg, "A review of methods used to determine the fractal dimension of linear features," Math. Geol. **26**, 23–46 (1994).

[22]R. Lopes and N. Betrouni, "Fractal and multifractal analysis: A review," Med. Image Anal. **13**, 634–649 (2009).

[23]B. H. Kaye, *A Random Walk Through Fractal Dimensions* (Wiley, 2008).

[24]H. O. Peitgen, H. Jurgens, and D. Saupe, *Chaos and Fractals: New Frontiers of Science* (Springer, 2004).

[25]B. Barnsley, *Fractals Everywhere* (Academic Press Professional, Inc., 2000).

[26]N. Sarkar and B. Chaudhuri, "An efficient differential box-counting approach to compute fractal dimension of image," IEEE Trans. Syst., Man, Cybern. **24**, 115–120 (1994).

[27]C. Chen, J. S. DaPonte, and M. D. Fox, "Fractal feature analysis and classification in medical imaging," IEEE Trans. Med. Imaging **8**(2), 133–142 (1989).

[28]M. Vegfors, L. G. Lindberg, P. Berg, and C. Lennmarken, "Accuracy of pulse oximetry at various haematocrits and during haemolysis in an in vitro model," Med. Biol. Eng. Comput. **31**, 135–141 (1993).

[29]A. G. Gilman, "G proteins: transducers of receptor-generated signals," Annu. Rev. Biochem. **56**, 615–649 (1987).

[30]M. Michalski, V. Briard, and F. Michel, "Optical parameters of milk fat globules for laser light scattering measurements," Lait **81**, 787–796 (2001).

[31]S. J. Sherwin and H. M. Blackburn, "Three-dimensional instabilities and transition of steady and pulsatile axisymmetric stenotic flows," J. Fluid Mech. **533**, 297–327 (2005).

[32]S. Kenjeres, "On recent progress in modelling and simulations of multi-scale transfer of mass, momentum and particles in biomedical applications," Flow, Turbul. Combust. **96**(3), 837–860 (2016).

[33]S. Kenjeres and A. de Loor, "Modeling and simulation of low-density-lipoprotein (LDL) transport through multi-layered wall of an anatomically realistic carotid artery bifurcation," J. R. Soc. Interface **11**(91), 1–13 (2014).